Available online at www.sciencedirect.com
SCIENCE DIRECT®
Journal of Magnetic Resonance 172 (2005) 333–341
JMR Journal of Magnetic Resonance
www.elsevier.com/locate/jmr

Aqueous flat-cells perpendicular to the electric field for use in electron paramagnetic resonance spectroscopy, II: design

Jason W. Sidabras[a], Richard R. Mett[a,b], James S. Hyde[a,*]

[a] Department of Biophysics, Medical College of Wisconsin, 8701 Watertown Plank Road, Milwaukee, WI 53226-0509, USA
[b] Milwaukee School of Engineering, Milwaukee, WI 53202-3109, USA

Received 27 August 2004; revised 1 November 2004
Available online 2 December 2004

Abstract

This paper builds on the work of Mett and Hyde [J. Magn. Reson. 165 (2003) 137]. Various aqueous flat-cell geometries in the perpendicular orientation have been studied using Ansoft High Frequency Structure Simulator (version 9.0, Pittsburgh, PA) and Computer Simulation Technology Microwave Studio (version 5.0, Wellesley Hills, MA). The analytic theory of Mett and Hyde has been refined to predict optimum dimensions of multiple sample cell structures including the effect of the sample holder dielectric properties and the interaction of the cells with each other on EPR signal strength. From these calculations and simulations we propose a practical multiple cell sample structure for use in commercial rectangular TE_{102} cavities that yields 2.0–2.3 times higher sensitivity relative to a single flat-cell in the nodal orientation. We also describe a modified TE_{102} resonator design with square rather than cylindrical sample-access stacks that is predicted to give a factor of 2.2–2.7 enhancement in EPR signal strength of a single flat-cell in the nodal orientation. These signal enhancements are predicted with sample holders fabricated from polytetrafluoroethylene. Additional improvement in EPR signal of up to 75% can be achieved by using sample holder materials with lower dielectric constants.

Keywords: EPR; Finite-element; Microwave cavities; Dielectric loss; Aqueous samples

1. Introduction

A conventional procedure for observation of aqueous EPR samples at X-band is to introduce the sample to a flat-cell cuvette that is placed in a rectangular TE_{102} cavity as shown in Fig. 1A. The cell lies in a nodal plane where the RF electric field intensity is zero and the RF magnetic field is maximum. Sample placement is very critical and only a few degrees of misalignment of the cell with respect to the x-axis results in a sharp decrease in the Q-value of the cavity. However, by rotating the cell precisely 90° from the so-called parallel orientation in the electric field node, Fig. 1A, to the perpendicular orientation, Fig. 1B, the Q-value recovers and good EPR signals can be obtained. Aqueous sample flat-cells oriented such that the RF electric field is perpendicular to the surface of the cell, Fig. 1B, were first studied by Hyde [1] and further discussed by Eaton and Eaton [2]. In both of these papers, experiments using more than one cell in perpendicular orientation were reported. More recently, Mett and Hyde [3] carried out a detailed theoretical analysis of the microwave fields when aqueous sample flat-cells are in the perpendicular orientation. They predicted that by placing multiple parallel flat-cells in a TE_{102} cavity with cell thickness (x-dimension), width (y-dimension), and the spacing between cells carefully optimized, a significant (3–6 times) EPR signal improvement can be achieved compared with a single optimized flat-cell in the parallel orientation of Fig. 1A.

* Corresponding author. Fax: +1 414 456 6512.
E-mail address: jshyde@mcw.edu (J.S. Hyde).

1090-7807/$ - see front matter © 2004 Elsevier Inc. All rights reserved.
doi:10.1016/j.jmr.2004.11.006

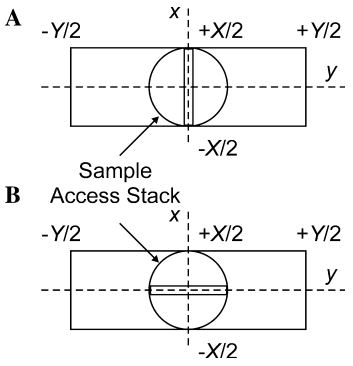

Fig. 1. Rectangular TE_{102} cavity cross-section. (A) Flat-cell in standard electric field nodal plane orientation. (B) Flat-cell in perpendicular orientation. The cavity dimensions are the same as the Varian Multipurpose resonator, $4.36 \times 1.02 \times 2.29$ cm, with a sample-access stack diameter of 1.1 cm.

The present paper builds on the analytic work of Mett and Hyde [3]. Extensive use is made of finite-element modeling of electromagnetic fields and analytic equations to calculate the optimum sample cluster dimensions. The analytic theory of Mett and Hyde [3] is extended and refined to make predictions of optimum sample cluster sizes and dimensions in the presence of a dielectric sample holder. Several practical multiple cell sample geometries are proposed for the X-band Varian Multipurpose TE_{102} cavity. Dimensions of this cavity are given in the caption of Fig 1. Extension to the similar Bruker cavity is straightforward.

Predicted EPR signals consistent with [3] were obtained using an assembly of identical flat-cells that extended from side-wall to side-wall when the relative dielectric constant of the sample holder was close to unity. These EPR signals were found to be 3.9–4.7 times that of a single flat-cell in standard orientation for 15–27 cells. We found that a sample holder of larger dielectric constant significantly lowered performance. For a polytetrafluoroethylene (PTFE) sample holder, the corresponding predicted EPR signal enhancement ratios were 2.2–2.7. We also found that the geometrical constraints imposed by the cylindrical 11 mm diameter sample-access stacks, see Fig. 1, further lowered performance by 8–24%, depending on the number of cells. Results using a 15-cell sample structure yielded about a factor of 2 better than the standard flat-cell geometry. Thus we propose a new TE_{102} resonator design with a square rather than circular sample-access stack, which is shown here to give a factor of 2.7 enhancement in EPR signal strength using a 27-cell sample assembly relative to the conventional flat-cell geometry of Fig 1A. Finally we consider the rectangular uniform field mode, TE_{U02}, [4–6] as well as the cylindrical TM_{110} cavity, both of which are compatible with aqueous sample flat-cell geometry in the perpendicular orientation [1].

Three types of power loss in an aqueous sample flat-cell were identified by Mett and Hyde, Types I, II, and III. Type I loss is the only type that is active in the parallel flat-cell geometry of Fig. 1A. There are no E_z components and negligible E_y components of the electric field, only E_x. All lines of RF electric field in the cavity are parallel to the flat-cell surface. The boundary condition at the cell surface is that the electric field tangential to the surface $\mathbf{E}_{\tan}$ be continuous across the surface. Power loss is determined by integration of E^2 within the sample volume. This geometry was analyzed by a number of workers in the early literature (see particularly Stoodley's paper [7]). It was recently reconsidered in the context of Uniform Field rectangular cavities in a paper from this laboratory [8].

All three types of power loss occur in the perpendicular orientation, Fig. 1B, and are defined below. Finite-element simulations that illustrate the electric fields giving rise to these sources of loss are shown in Fig. 2. The sample boundary is outlined in black in this figure, and the relative dielectric constant of the sample holder is unity. Dimensions of the sample cell are $0.4 \times 8 \times 22.9$ mm, which are the same as commercial cells for use in the geometry of Fig. 1A. Fig. 2A shows the electric field magnitude in an x–y plane with the nodal electric field null portrayed as a dark blue band. The flat-cell is perpendicular to the nodal plane. Fig. 2B shows only the component of electric field perpendicular to the surface, E_x, in an expanded view, while Figs. 2C and D show the electric field tangential to the surface, E_y.

A major and perhaps surprising finding of Mett and Hyde [3] was that Type I loss exists when the flat-cell is in the perpendicular orientation, which requires that E_y be non-zero. This component of the RF electric field is strictly zero in the empty cavity. The existence of non-zero E_y is understood as follows: polarization charges terminate the lines of RF electric field in the x-direction because of the discontinuity in E_x occurring at the sample surface, noting the high dielectric constant of water. Because E_x changes approximately linearly along the sample in the y-direction, the density of polarization charges also changes approximately linearly in the y-direction along the surface of the sample. This gives rise to a component of $\mathbf{E}$ along y, and thus to Type I loss. For this effect to occur, it is necessary that $\partial E_x/\partial y > 0$—that the sample lie in a gradient of the RF electric field.

Fig. 2C shows that the polarities of E_y on either side of the sample are opposite creating a zero at the center of the sample slab (green color). A major finding of Mett and Hyde [3] is that tangential electric field nulls exist within each cell in the multiple cell configuration. Fig. 2C also shows that E_y peaks half way between the y-edges of the sample with a maximum value occurring at $y = 0$, which is the nodal plane for E_x and the point of maximum gradient in E_x.

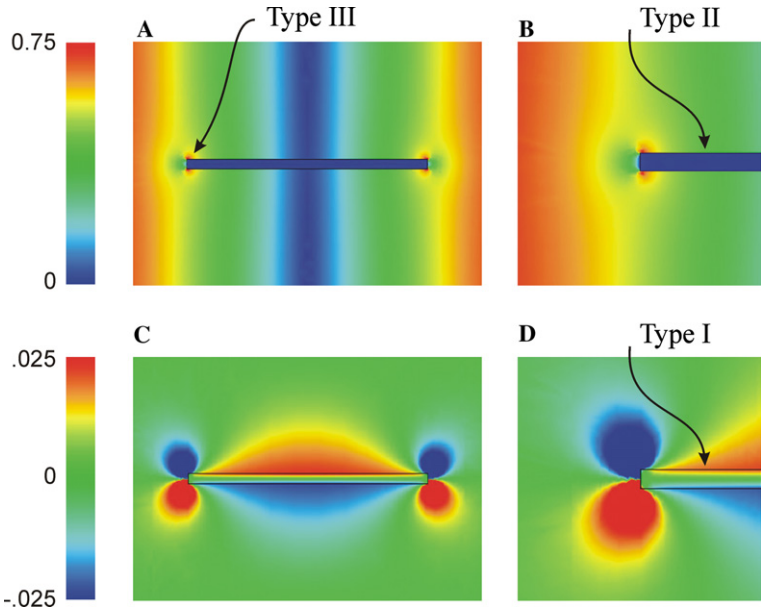

Fig. 2. Spatial electric field profiles in the x–y plane for the sample of Fig. 1B showing three EPR signal loss types. (A) Magnitude of the electric field E showing Type III loss, which is associated with partial electric field cancellation at the end of the sample. (B) Electric field in the x-direction E_x showing Type II loss which is associated with the perpendicular electric field within the sample. (C) Electric field in the y-direction E_y showing Type I loss, which is associated with the tangential electric field within the sample. (D) Expanded view of (C).

Type II loss can be seen in Fig. 2B. Although E_x is discontinuous at the sample surface because of the high dielectric constant of water and is greatly reduced inside the sample, it nevertheless has a finite value and results in loss. There is a small variation of E_x across the sample thickness predicted by the analytical equations of Mett and Hyde [3]. It is an effect that depends on the wavelength in water at X-band. When optimum, Type I loss plus the cavity wall power loss is approximately equal to the Type II loss when the samples are in the perpendicular orientation as predicted in Mett and Hyde.

Type III loss refers to the regions of complexity at the edges of the sample where local electric field intensities become quite high. Polarization charges on opposite corners of an edge give rise to electric field vectors that tend to oppose the applied electric field in free space. Nevertheless, there is a residual component of E_x at the edge that penetrates the sample because it is tangential to the edge surface. This penetration increases the total electric field in the sample near the edge about two times relative to what would be expected from Type II loss alone. Type III loss was analyzed extensively by Mett and Hyde [3].

2. Methods

The results of this paper are based on finite-element simulations of electromagnetic fields. Two commercial programs were available to us: Ansoft High Frequency Structure Simulator (HFSS) (version 9.0, Pittsburgh, PA) and Computer Simulation Technology (CST) Microwave Studio (version 5.0, Wellesley Hills, MA). Both programs permit "driven mode" and "eigenmode" solutions of Maxwell's equations. The eigenmode method was used exclusively in the work described here. Although these programs are similar, they differ in a number of respects including (i) methods to create the finite-element mesh, (ii) the drawing package describing the microwave structure, and (iii) graphic display options.

Two computers were used, Compaq W8000 workstation with dual Xeon 1.7 GHz processors with 4 GB of RAM and HP workstation xw8000 with dual Pentium Xeon 3.2 GHz processors with 1 MB of cache and 4 GB of RAM. The operating system was Windows 2000 for both computers. The newer 3.2 GHz computer was benchmarked at about two times faster performance than the older 1.7 GHz model in this application.

All simulations were done at X-band (9.5 GHz) for aqueous samples in a rectangular TE_{102} cavity made from copper. Dimensions are given in the caption of Fig. 1. The relative dielectric constant of water at 10 GHz and 25 °C was taken as $\varepsilon_{rs} = 55(1 + 0.54i)$ [9]. Some simulations were with no sample holder; other simulations included the effect of a sample holder made of PTFE, $\varepsilon_{rh} = 2.08(1 + 3.7 \times 10^{-4}i)$ [9].

In all cases, the EPR sample was considered to be saturable with the available microwave power. For this class of samples in EPR spectroscopy, experimental comparisons between resonator geometries are made by readjusting the incident power such that the peak value of the microwave RF magnetic field in the region of the sample is held constant [8,10]. Experimentally, the EPR spectroscopist typically determines $P_{1/2}$, the value

of the incident microwave power where the signal intensity is half of what it would be if no microwave power saturation occurred. The power is then reduced by a fixed amount in order to avoid significant microwave power saturation of the sample. It is then assumed that the experimental signal intensity is an integration of the contributions of all spins over the cosine distribution of H_1 along the sample and that none of these spins exhibit significant microwave power saturation. It is this experimental procedure that is duplicated in the simulation and analysis of fields.

In the eigenmode solution method, HFSS sets the most intense electric field magnitude to 1 V/m, while the CST software assumes 1 W of power is feeding the structure. Neither program directly permits normalizing the RF magnetic fields, but both programs allow integration of peak magnetic field energy stored in the sample and in the cavity. Using Eqs. (31)–(40) of [3], it is straightforward to derive Eq. (1), which can be used with both HFSS and CTS to compare signal intensities for saturable samples.

$$S_{\mathrm{sat}} = \frac{\mu_0 \pi f}{\mu_0 10^4 H_{\mathrm{m}}} \frac{\int H_{\mathrm{s}}^2 \, \mathrm{d}V_{\mathrm{s}}}{\sqrt{P_l}}. \tag{1}$$

Here, f is the frequency, μ_0 is the magnetic permeability, H_{m} is the magnitude of the maximum magnetic field within the cavity (A/m), H_{s} is the magnetic field within the sample, and P_l is the power input into the cavity. In this equation the units of the numerator and denominator are Joules and Gauss, respectively. The power into the cavity can be found from

$$P_l = \frac{2\pi f U_{\mathrm{c}}}{Q_l}, \tag{2}$$

where U_{c} is the stored energy within the cavity and Q_l is the loaded quality factor of the cavity.

A possible concern in the simulations is the assumption of ideal sample cells with sharp interior corners and uniform wall thickness, planarity, and spacing. We have a high level of confidence in the simulations, and would attribute any difference between actual and predicted performance to a failure to model the actual structure. Fully rounding the inner corners of a standard flat-cell was found to decrease the predicted EPR signal by only 0.2%.

3. Results

3.1. Single-cell to n-cell analysis

A major finding of Mett and Hyde [3] is that each individual sample cell has a tangential electric field node within it. Sample cell placement within the cavity was found to have a major influence on the position of this node. Because of the linear variation of the tangential electric field within the sample, Type I loss is four times smaller if the node is perfectly centered within the sample than if the node is on the sample surface. This factor of four reduction in dielectric loss results in a significant enhancement in the EPR signal strength, Eq. (1).

The EPR signal strength normalized to unity at the cavity center ($x = 0$) is shown in Fig. 3 as a function of the x-sample position b for a single sample in perpendicular orientation. The solid line is for sample width of 8 mm. The signal is constant until the sample gets quite close to the cavity wall. As the sample approaches the wall, the tangential electric field null shifts off-center, increasing the loss and decreasing the EPR signal strength. When the sample is on the wall, the signal strength is lower by nearly 30%. This is because the Type I losses have quadrupled since the null is not centered in the sample, while the Type II loss and cavity wall loss have remained constant. At optimum signal, Type I loss is comparable to the cavity wall losses plus Type II loss [3]. The dashed line of Fig. 3 is for a sample width of 4 mm. In this case, the tangential electric field peak is reduced, which allows the sample cell to approach the wall more closely before the tangential electric field null is moved off-center. Although decreasing the sample width Y_{s} is beneficial in reducing the effect of nearby boundaries, it also can produce a non-optimum cell dimension that lowers the EPR signal.

Mett and Hyde [3] found that to reduce power losses one could divide the sample cell into multiple cells. Maximum reduction of the tangential electric field for an optimum sample thickness and number of cells is achieved when the tangential electric field null is centered within each sample. The location of this null depends on the positioning of the cells within the cavity. Using Ansoft HFSS, it was found that uniform cell-to-cell spacing and half-spacing from an edge-cell to the cavity wall produces perfect centering of the tangential

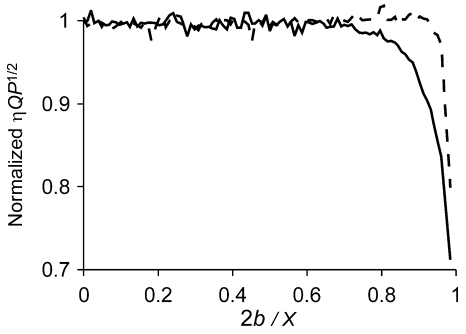

Fig. 3. EPR signal strength normalized to unity at the cavity center as a function of cell position, b, for a single cell in perpendicular orientation. The solid line is for a cell of standard dimensions, and the dashed line is for a cell of half the standard width. The numerical noise in the data comes from the finite-element simulations.

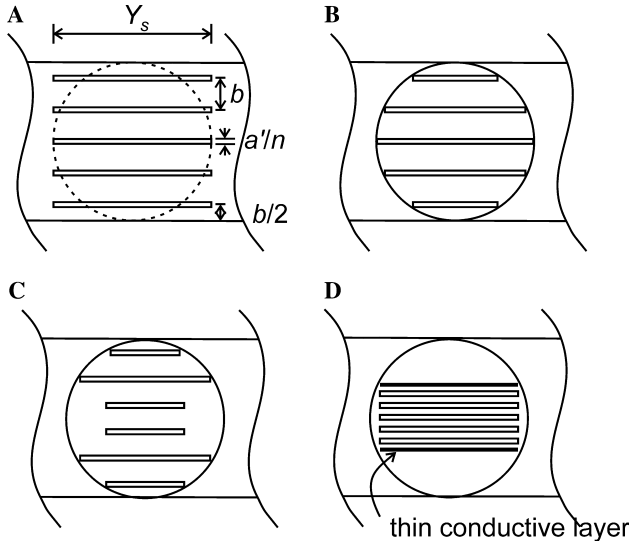

Fig. 4. Cell configurations relative to the sample-access stack. (A) A TE_{102} cavity with sample cluster of ideal spacing, thickness, and width. (B) Circular sample cluster achieved by varying the Y_s of the cells to conform to the sample-access stack. (C) Figure-8 sample cluster, which results in improved centering of tangential electric field nulls within the sample cells. (D) A practical sample structure for use with circular sample-access stack. Conducting sheets are used to establish perpendicular boundary conditions at the top and bottom of the cells.

electric field nodes within each sample. This spacing is shown in Fig. 4A. Clustering of cells in the center of the cavity with uniform cell-to-cell spacing did not produce satisfactory signal gains. In this case, the tangential electric field nodes are centered in each sample for the middle cells in the cluster, but not for the cells near the edges of the cluster [11].

3.2. Sample cluster optimization

The optimum sample-cell cluster dimensions predicted by Mett and Hyde as shown in Table 1 of [3] were used in finite-element simulations. These analytical results were based on field solutions for a one-celled structure and scaled to multiple cells. A comparison of EPR signal strength ratios of multiple cells to a standard single-cell in parallel orientation showed that the ratio was 20–30% lower in the simulations than predicted analytically. This was found to be caused by inadequacies in the scaling method.

An analytical method to correct this deficiency has been found. Using the integral form of Faraday's Law, one can derive an accurate dependence of the perpendicular electric field of a sample cell within a cluster, E_{xsn}, to that of a single isolated cell, E_{xs1}. The path of integration is from $(-X/2, y, 0)$ to $(X/2, y, 0)$, a distance y from the nodal plane. The closed path is completed along the cavity wall and down the nodal plane. These segments do not contribute to the line integral. If the magnetic field strength at the center of the resonator is the same with one sample of thickness a' as it is with n samples, each with a thickness a'/n, and y is relatively small, $y \ll Y_s/2$, the flux enclosed by the enclosed path is the same for the two cases. This allows one to relate the perpendicular electric fields:

$$\frac{E_{xsn}}{E_{xs1}} \cong \varepsilon_{\mathrm{rh}} \Big/ \left(1 - \frac{a'}{X}\left(1 - \frac{\varepsilon_{\mathrm{rh}}}{\varepsilon_{\mathrm{rs}}}\right)\right), \tag{3}$$

where a' is the total thickness of the sample cluster, $\varepsilon_{\mathrm{rs}}$ is the real part of the dielectric constant of the sample, and $\varepsilon_{\mathrm{rh}}$ is the real part of the dielectric constant of the sample holder, which, if present, is assumed to extend fully across the cavity x-dimension. It can be seen that the perpendicular electric field is increased by both more sample a' in the resonator and increased dielectric constant of the sample holder. A similar relationship between tangential electric field components can be formulated by considering how the magnitude of the surface polarization charge depends on the perpendicular electric field,

$$\frac{E_{\tan sn}}{E_{\tan s1}} \cong \frac{1}{1 - a'/X}. \tag{4}$$

Eqs. (3) and (4) can be used to correct the constants C_2 and C_3 which were developed in Section 3.4.2 of the analytic theory of Mett and Hyde [3] to predict the optimum

Table 1
Comparison of EPR signal strengths with (shaded) and without PTFE used as a sample holder

Sample number n	Individual cell thickness a'/n (mm)	Sample width Y_s (cm)	Signal strength $S_{\mathrm{sat}} = \eta Q_l P_{\mathrm{in}}^{1/2}$	Signal ratio over single cell in standard orientation SR_{sim}	Percent difference of signal ratio from analytical results $\frac{SR_{\mathrm{sim}} - SR_{\mathrm{an}}}{SR_{\mathrm{sim}}} \times 100\%$	Resonator frequency (GHz)	Sample volume (μL)	Q_l
1 (nodal)	0.400	0.80	14.4	1	0.0	9.49	73.3	1830
15	0.156	1.27	56.1	3.89	4.9	9.28	681	584
	0.185	0.603	31.3	2.18	−0.5	9.28	383	480
15 (Fig. 4D)	0.133	1.30	48.2	3.35	−1.5	9.26	548	466
	0.151	0.610	28.9	2.00	2.5	9.32	316	538
19	0.138	1.20	60.6	4.20	7.1	9.28	721	599
	0.158	0.603	33.8	2.34	2.6	9.27	415	472
27	0.108	1.13	67.0	4.65	9.0	9.28	755	656
	0.121	0.603	38.0	2.64	10.2	9.26	451	502

sample cluster dimensions for maximum EPR signal strength. The replacements read

$$C_2 \rightarrow C_2\left[\varepsilon_{\mathrm{rh}}\Big/\left(1-\frac{a'}{X}\left(1-\frac{\varepsilon_{\mathrm{rh}}}{\varepsilon_{\mathrm{rs}}}\right)\right)\right]^2, \tag{5}$$

$$C_3 \rightarrow C_3\left(\frac{1}{1-a'/X}\right)^2. \tag{6}$$

To fully account for the dielectric of the sample holder, an additional scaling must be made to account for the shortening of the wavelength in the y-direction within the sample holder dielectric relative to that of free space [12]. This wavelength shortening is predicted by the dispersion relation within the sample holder dielectric,

$$\frac{4\pi^2 f^2}{\varepsilon_{\mathrm{rh}} c^2} = k_x^2 + k_y^2 + k_z^2, \tag{7}$$

where c represents the speed of light in vacuum and k is the wavenumber. The increased variation of electric field with y is carried into the sample. By reducing the sample width Y_{s} predicted by the analytic theory as

$$Y_{\mathrm{s}} \rightarrow Y_{\mathrm{s}}/\sqrt{\varepsilon_{\mathrm{rh}}}, \tag{8}$$

an optimum sample size was found.

The analytic theory of Mett and Hyde was modified according to Eqs. (5), (6), and (8), and more accurate optimum sample cluster dimensions were predicted. For low sample holder dielectric constant, the new predicted optima have larger sample widths and smaller thicknesses than the original analytic theory due to the increased electric field within the sample. For higher values of dielectric constant, the optimum sample widths decrease and the thicknesses increase.

Ansoft HFSS was used to calculate the EPR signal strength for the predicted optimum sample cluster dimensions from the new analytic model for 15-, 19-, and 27-cell clusters. Results for a sample holder with a dielectric constant of free space are shown as the non-shaded entries in Table 1. Significant EPR signal enhancement factors of 3.9–4.7 are shown. In these cases, signal strength was observed to continue to increase slowly with sample width with a corresponding decrease in Q_l, consistent with the observations of Mett and Hyde [3]. The optima were chosen to correspond to a practical microwave bridge-limited Q_l value of approximately 500. The optima were confirmed by simulating sample clusters with 5% variations in total sample thickness and width. The EPR signal was observed to decrease in all cases.

The effects of the number of cells on the electric fields are plotted in Fig. 5. Holding Y_{s} constant, all cell thicknesses have been optimized for maximum EPR signal strength for the given number of cells. One cell (A), three cells (B), and nine cells (C) are shown. The first column (i) shows the x-dependence of the tangential electric field E_y in the center of the cavity on the nodal plane of the perpendicular electric field E_x. In each case (A), (B), and (C), the tangential electric field nodes are centered within each cell, minimizing the Type I loss. The second column (ii) shows the x-dependence of the perpendicular electric field at a y-position away from the nodal plane of E_x. The y-position is 2/3 of the distance from the center to the edge of the sample such that there is significant perpendicular electric field, but little contribution from Type III losses. Column (ii) shows a progressive increase in the perpendicular electric field with the number of samples. The third column (iii) shows the y-dependence of the perpendicular electric field along the sample width. The linear variation in the center region is Type II loss and the near-doubling of the field magnitude in the vicinity of the sample edge is Type III loss. In row (D) of Fig. 5, a three-celled structure is shown where the cells are spaced too closely together. In column (i) the vertical lines represent the center of the sample, where the tangential electric field strength has the same magnitude as the tangential electric field strength for a one sample case. But the tangential electric field nulls are not centered in the sample cells. In column (ii), the perpendicular electric fields are larger when the cell spacing is smaller, increasing the losses within the sample. These effects decrease the Q and EPR signal strength.

3.3. Cluster design to fit the circular sample-access stack

As a first step in the design of a practical multi-cell sample structure, the assumption was made that the dielectric constant of the sample holder is unity and that it should fit the existing Varian Multipurpose TE_{102} resonator depicted in Fig. 1. Dimensions must permit insertion though the sample-access stack of 11 mm diameter. A naive approach is to place cells of varying widths along the entry stack as shown in Fig. 4B. This configuration does not produce tangential electric field nulls that are centered in all cells, increasing the dielectric losses and degrading the EPR signal. This effect can be corrected somewhat by reducing the amount of sample in the center of the cavity, resulting in the figure-8 sample configuration shown in Fig. 4C. In this configuration, Type II losses are reduced, and some improvement in the null centering is observed. A gain of about 1.5 in signal strength over the circular structure of Fig. 4B is obtained using the figure-8.

A better approach is to place a thin layer of conducting material along each x-boundary of the sample cluster as shown in Fig. 4D. Since the x-dimension of the TE_{102} cavity is a free parameter, conducting plates can be added to the sides of the sample cluster without significantly distorting the rectangular TE_{102} mode fields. The electric field is perpendicular at these conducting boundaries. Cells are spaced uniformly apart between the conducting plates. The new optimum sample thick-

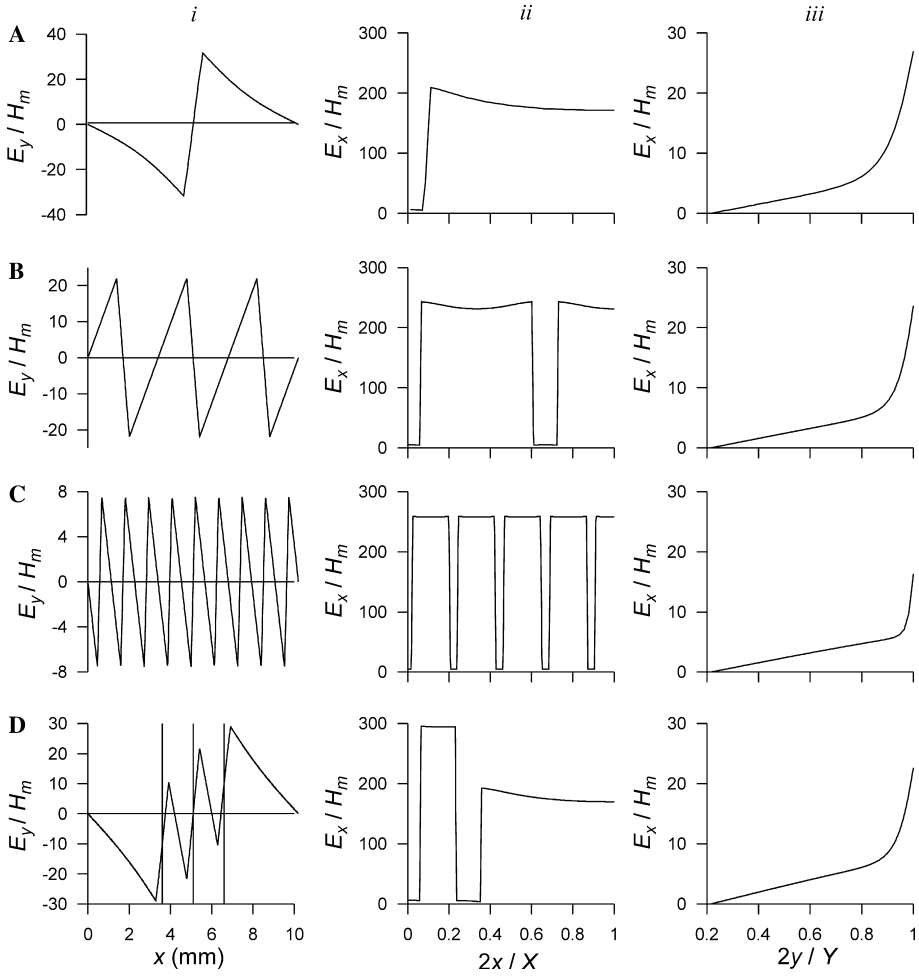

Fig. 5. Perpendicular and tangential electric fields (V/m) normalized to the magnetic field H_m (A/m) in the cavity center. Rows (A), (B), and (C) correspond to increase in number of sample cells for ideal spacing, $n = (A)\ 1, (B)\ 3, (C)\ 9$ sample cells, and row (D) for 3 cells with non-ideal spacing. Columns (i) and (ii) show the tangential and perpendicular electric fields, respectively, across the sample thickness, while Column (iii) shows the variation of the perpendicular electric field across the sample width.

ness and width for 15 cells are found with the analytic theory of Section 3 using a cavity with x-dimension equal to the distance between the conducting plates, $X = 0.735$ cm. The finite-element simulation with the full-size cavity and the sample insert yields EPR signals approximately equal to those predicted by the analytic theory as shown in Table 1. The 15-cell cluster has an EPR signal 3.4 times that of the standard flat-cell.

Adding the conducting plates to the sample cell cluster increases the electric field across the sample region compared to that outside the cluster. The magnetic field within the sample is correspondingly increased through $\nabla \times E$. This enhancement of the magnetic field increases the filling factor and the overall EPR signal over what would be expected if the magnetic field were the same inside and outside the cluster. As the distance between conducting plates X_c approaches the cavity wall dimension X, this effect becomes less pronounced. It was found that limiting X_c to no more than $\frac{3}{4}X$ produces a satisfactory EPR signal enhancement. Conducting plates are helpful when the sample cluster is not oriented exactly 90° with respect to the nodal plane.

3.4. Use of PTFE as a sample holder material

Up to this point, we have considered a sample holder that has the dielectric constant of free space. We now model the sample holder using the dielectric constant of PTFE. A dielectric sample holder produces an increase in the perpendicular electric field strength inside the sample by a factor of ε_{rh} as shown by Eq. (3), whereas the tangential electric field strength is not changed by the dielectric properties of the sample holder, Eq. (4). There is also a reduction in the sample width, Eq. (8). The shaded entries in Table 1 show Ansoft HFSS simulations using 15-, 19-, and 27-celled structures with a sample holder made of PTFE. The dielectric fills all regions between sample cells in the x-dimension and extends 0.3 mm beyond the sample width boundary on both sides of the sample giving the sample holder dimen-

sions of (X, $Y_s + 0.6$ mm, L). There is uniform cell-to-cell spacing and half-spacing from an edge-cell to the conducting wall. Sample thicknesses and scaled widths predicted to be optimum by the analytic theory are shown, Table 1. Significant signal enhancement ratios of 2.0–2.7 are indicated.

Finite-element simulations verified that when PTFE is introduced, the perpendicular electric field within the sample increases. In Fig. 6, the perpendicular electric field in a nine-celled structure with and without PTFE sample holder is shown. There is an increase in E_x within the sample by approximately ε_{rh} (A) and (B). Calculations of the integral of E^2 over the sample volume showed that reducing Y_s by $\sqrt{\varepsilon_{rh}}$ reduces the dielectric losses to values comparable to those with a sample holder of free space.

With the adjustments of Y_s, the conductive boundary of Fig. 4D with a PTFE sample holder is practical. A factor of 2.0 improvement in EPR signal strength over the standard flat-cell in the nodal position was found. Similar adjustments for the figure-8 configuration of Fig. 4C yielded little recovery in EPR signal after the addition of PTFE due to the lack of centering of the tangential electric field nodes.

Further EPR signal improvement over the multi-celled sample structure of Fig. 4D is possible with the design of a new TE_{102} cavity containing a square sample-access stack. Such a structure is shown in Fig. 4A and results in a factor of 2.2–2.7 or greater increase in signal strength depending on the practicality of extrusion techniques, the number of cells and the Q factor. Introducing a square sample-access stack will allow ideal placement of cells perpendicular to the cavity walls. This also will allow easier alignment of the sample stack. Another benefit of a new resonator design is the opportunity to increase the x-dimension of the resonator. Increasing X permits more sample cells to be placed in perpendicular orientation, increasing the EPR signal strength.

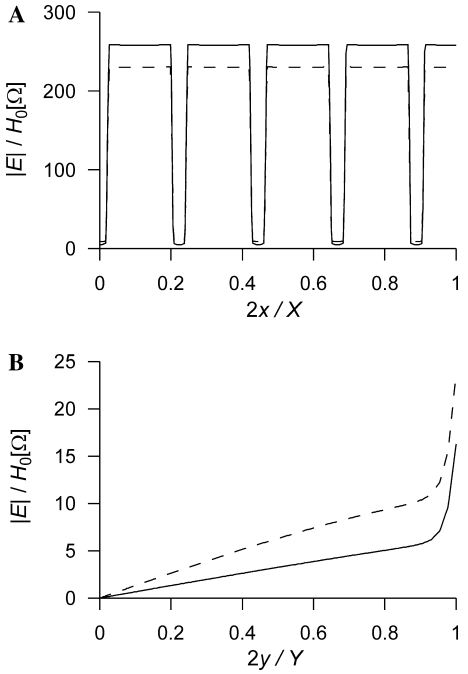

Fig. 6. Comparison of electric field with a sample holder dielectric constant of free space (solid) and PTFE (dashed) for a given magnetic field H_m in the cavity center. (A) Perpendicular electric field for a nine-celled structure. (B) Perpendicular electric field variation across the sample width.

It is important for the spectroscopist to know the effect of the perpendicular orientation on the uniformity of the RF magnetic field. Calculations using Ansoft HFSS show a maximum of the magnetic field in the center of the sample cluster near the electric field nodal plane and a decrease in magnetic field strength with distance along y. For optimum sample cluster dimensions, the magnetic field strength decreases by about 35–45% from the center to the edge of the sample. The larger percentage occurs with a PTFE sample holder.

4. Other resonator types

Other resonator types, such as the uniform field resonator [4–6] developed in this laboratory, have been considered. The uniform field resonator is desirable for EPR spectroscopy because the RF magnetic field is uniform along two free dimensions X and L (the cavity central section z-dimension) and saturates the sample evenly. The multiple sample analysis done here and in Mett and Hyde [3] carries over to the uniform field resonator without modification. Around a 10% reduction in EPR signal strength is seen with the U02 mode resonator caused by the more rapid variation in fields in the y direction. This signal reduction is compensated by the uniformity in magnetic field in z and can be more than regained by increasing L.

Another mode that was considered is the cylindrical TM_{110} cavity. This mode is analogous to the rectangular TE_{102} in that the electric fields lie along x and have two opposing regions of concentration separated by a nodal plane. The magnetic field patterns are also similar. The analysis of the paper carries over to this mode without much modification, allowing a change in optimum Y_s because of the geometrical differences between a TE_{102} and a TM_{110} cavity.

5. Conclusions

The multiple flat-cell clusters in perpendicular orientation proposed by Mett and Hyde [3] have been simulated and analyzed with the use of finite-element codes. Modifications of the analytic theory of Mett and Hyde [3] that include the effects of the sample holder dielectric and the interaction of the cells with each other

resulted in improved predictions of optimum flat-cell cluster dimensions. The analysis resulted in sample clusters that produce gains of 2.0–2.7 times the EPR signal strength over the standard flat-cell in parallel orientation [13]. Further increases in signal are possible by using larger numbers of sample cells, but fabrication of the sample holder becomes difficult. Additional increases in signal of up to 75% are also possible by using a sample holder dielectric material with lower dielectric constant.

The perpendicular electric field in the sample cells is increased by the interaction of the cells with each other and by the dielectric properties of the sample holder, Eq. (3). The tangential electric field strength is only influenced by the number and thickness of cells, Eq. (4). The sample holder also shortens the wavelength across the sample width by $\sqrt{\varepsilon_{\mathrm{rh}}}$, Eq. (8). All of these physical effects strongly influence the optimum sample dimensions.

Using the commercial rectangular TE_{102} cavity with a circular 11 mm sample-access stack, and limiting the number of sample cells to 15, a factor of 2 in EPR signal strength over the standard flat-cell can be achieved. This sample cluster is sandwiched between two metallic plates, which produce a symmetric field pattern between them. A rectangular TE_{102} cavity with a square sample-access stack would yield a further improvement of EPR signal of 2.2–2.7 over the standard flat-cell. This sample cluster does not require the metallic shields.

Acknowledgments

This work was supported by Grants EB001417 and EB001980 from the National Institute of Biomedical Imaging and Bioengineering of the National Institutes of Health.

References

[1] J.S. Hyde, A new principle for aqueous sample cells for EPR, Rev. Sci. Instrum. 43 (1972) 629–631.
[2] S.S. Eaton, G.R. Eaton, Electron paramagnetic resonance sample cell for lossy samples, Anal. Chem. 49 (1977) 1277–1278.
[3] R.R. Mett, J.S. Hyde, Aqueous flat cells perpendicular to the electric field for use in electron paramagnetic resonance spectroscopy, J. Magn. Reson. 165 (2003) 137–152.
[4] R.R. Mett, W. Froncisz, J.S. Hyde, Axially uniform resonant cavity modes for potential us in electron paramagnetic resonance spectroscopy, Rev. Sci. Instrum. 72 (2001) 4188–4200.
[5] J. Anderson, R.R. Mett, J.S. Hyde, Cavities with axially uniform field for use in electron paramagnetic resonance. II. Free space generalization, Rev. Sci. Instrum. 73 (2002) 3027–3037.
[6] J. Hyde, R. Mett, J. Anderson, Cavities with axially uniform field for use in electron paramagnetic resonance. III. Re-entrant geometries, Rev. Sci. Instrum. 73 (2002) 4003–4009.
[7] L.G. Stoodley, The sensitivity of microwave electron spin resonance spectrometers for use with aqueous solutions, J. Electron. Control 14 (1963) 531.
[8] J.S. Hyde, R.R. Mett, Aqueous sample considerations in uniform field resonators for electron paramagnetic resonance spectroscopy, Curr. Top. Biophys. 26 (2002) 7–14.
[9] A. Von Hippel, Dielectric Materials and Applications, Artech House, Boston, 1954.
[10] J.S. Hyde, W. Froncisz, Loop-gap resonators, in: A.J. Hoff (Ed.), Advanced EPR: Applications in Biology and Biochemistry, Elsevier, Amsterdam, 1989, pp. 277–306.
[11] A coding error in Mett and Hyde [3] led to the conclusion that a closely-packed cell cluster would produce optimum tangential electric field node centering in the cells. This error is manifest in Fig. 3E of [3] and was caused by a sign error in programming. All equations and all other graphs in [3] are believed to be accurate.
[12] Here, we hold the resonator dimensions fixed and assume that the dielectric of the sample holder does not have a significant effect on the resonant frequency. As indicated in Table 1, the largest frequency shift caused by the Teflon sample holder is less than 1%.
[13] In the rectangular TE_{102} cavity, a standard flat-cell in nodal orientation has 4.1 times the signal of a standard capillary of 1.1 mm diameter, neglecting the effects of the sample holder dielectrics.